Energy Conversion and Management 103 (2015) 459–467

Contents lists available at ScienceDirect

Energy Conversion and Management

journal homepage: www.elsevier.com/locate/enconman

Gray-box model for energy-efficient selection of set point hysteresis in heating, ventilation, air conditioning, and refrigeration controllers

M.A. Fayazbakhsh, F. Bagheri, M. Bahrami *

Laboratory for Alternative Energy Conversion, School of Mechatronic Systems Engineering, Simon Fraser University, 250-13450 102 Avenue, Surrey, BC V3T 0A3, Canada

ARTICLE INFO

Article history:
Received 18 April 2015
Accepted 23 June 2015
Available online 8 July 2015

Keywords:
HVAC–R
On/off controller
Set point hysteresis
Energy efficiency
Gray-box model

ABSTRACT

Many heating, ventilation, air conditioning, and refrigeration systems operate using on/off controllers. A high and a low set point are selected above and below the desired temperature to command the refrigeration cycle to turn on or off when those temperatures are reached. In this study, exponential temperature correlations are used in a gray-box approach to provide information about the estimated mean temperature, average power consumption, and number of compressor starts per hour. Based on the governing equations and the heat balance of the system, a set of formulations is developed as a new analytical tool for the design of set points. It is discussed that for any specific application, the set point values can be properly selected to minimize the overall energy consumption subject to the design constraints. It is shown through an experimental study that the selection of the set points can affect the overall energy consumption by up to 49% for the same desired temperature. It is also shown that there is a further opportunity for increasing the energy efficiency by 6.6% using different high and low set point hysteresis values. The developed model can be used for designing and analyzing new systems. It can also be used for retrofitting existing units and achieving the highest energy efficiency subject to the design constraints.

1. Introduction

Half of the total energy used in buildings and 20% of the total national energy used in European and American countries is consumed by Heating, Ventilation, Air Conditioning, and Refrigeration (HVAC–R) systems [1]. HVAC–R energy consumption can exceed half of the total energy usage of a building located in tropical climates [2]. Furthermore, industrial refrigeration systems consume a substantial amount of energy. Supermarket refrigeration systems, for instance, may use up to 80% of the total energy consumed in the supermarket [3].

Moreover, Air Conditioning (AC) is a significant energy consuming unit in vehicles [4]. For a typical vehicle under peak load, the AC energy usage outweighs the energy loss to aerodynamic drag, rolling resistance, and driveline losses, combined [5]. AC can reduce the fuel economy of mid-size vehicles by more than 20% and it can also increase vehicle NOx and CO emissions by approximately 80% and 70%, respectively [6]. Around 7 billion gallons of fuel are consumed annually by the AC systems of light-duty vehicles in the United States [7]. Hence, reduction of fuel consumption and tailpipe emissions are two crucial goals for the auto industry that can be achieved by more efficient designs of mobile AC systems.

Controller design is a critical aspect of HVAC–R systems. Proper selection and design of the controller directly affects the overall energy consumption and thermal comfort. Air conditioning and refrigeration systems are often controlled by feedback systems that receive input signals from a temperature sensor such as a thermocouple installed inside the conditioned space. The controller compares the measured temperature to the desired (set point) temperature, and provides an output to the control element. The control element of the refrigeration system can be the compressor, the evaporator fan(s), or the condenser fan(s). The controller is an integral part of the HVAC–R system, thus the entire system should be analyzed to select a proper and efficient controller.

The design methodology for HVAC–R controllers can be categorized with respect to their reliance on real-time data measurements. White-box (purely law-driven), black-box (purely data-driven), and gray-box (combination of the two) modeling approaches are among the methods proposed in the literature [8]. White-box methods are purely based on predetermined physical laws and are unaware of the real-time operation of the system. Black-box methods are learning algorithms that are often designed as generic tools for intelligent control systems regardless of the actual application. Gray-box approaches offer a mix of the two.

* Corresponding author. Tel.: +1 (778) 782 8538; fax: +1 (778) 782 7514.
E-mail address: mbahrami@sfu.ca (M. Bahrami).

http://dx.doi.org/10.1016/j.enconman.2015.06.071
0196-8904/

Nomenclature

c	specific heat (J/kg °C)
c_1	parameter of the temperature correlation (°C)
c_2	parameter of the temperature correlation (°C)
c_3	parameter of the temperature correlation (s)
h	convection heat transfer coefficient (W/m^2 °C)
H	representative parameter of heat generation (W)
m	mass (kg)
$\dot{m}$	mass flow rate (kg/s)
M	representative parameter of thermal inertia (J/°C)
n	number of compressor starts per hour (1/h)
P	effective compressor power consumption (W)
P_{comp}	approximate compressor power consumption when on (W)
$\dot{Q}$	heat transfer rate (W)
R^2	coefficient of determination
S	surface area (m^2)
t	time (s)
T	temperature (°C)
U	representative parameter of heat transfer (W/°C)

Subscripts and superscripts

0	initial value at the beginning of a process
a	room air
c	calculated value based on piecewise exponential temperature correlations
D	temperature-decreasing process
g	internal heat generation
H	high set point
$HVAC$	HVAC source
i	wall number
I	temperature-increasing process
L	low set point
m	mean value over a temperature swing
o	outside air
s	surface
v	ventilation and infiltration

In gray-box methods, the governing equations of the specific control problem is incorporated in the design to some extent, while available operation data are also utilized to complement the approach with a degree of real-time intelligence. In the following section, an overview of the existing HVAC–R control methods is provided.

1.1. HVAC–R controllers

A wide spectrum of controller types is available for HVAC–R applications. Classic controllers include: on/off, proportional, and PID controllers. Although more sophisticated controllers are being made available, the industry often delays adopting the new methods due to the associated cost, complexity, and lack of incentives. It is therefore important to consider approaches that can be adopted rather quickly with utmost ease and tolerable cost.

On/off controllers are capable of switching the system on and off based on a comparison between the measured temperature and the desired set point. On the other hand, proportional and PID controllers are meant for systems that have the capability of varying the provided heating/cooling power. For instance, a PID controller not only switches a heater on or off, it can also control the amount of heating energy input to the room. Therefore, proportional or PID controllers are generally more desirable for variable-capacity systems. One issue with adopting a conventional PID controller is the selection of its coefficients, which is often determined through measurements. Wemhoff [9] proposed a simple calibration procedure for successive optimization of the proportional, integral, and derivative coefficients to reduce energy consumption. Similar optimization concepts are applicable to the set points in on/off controllers [10]. Due to the higher initial cost associated with variable-speed compressors and fans, on/off control and constant capacity components are more common in HVAC–R applications.

Artificial intelligence approaches for HVAC–R control include neural networks, genetic algorithms, and fuzzy logic which suggest new frontiers of HVAC–R control beyond the classic methods. Mirinejad et al. [11] recently conducted a thorough review of intelligent control techniques used in HVAC–R systems.

Neural networks are being widely used to establish load prediction algorithms. Li et al. [12] presented four modeling techniques for hourly prediction of thermal loads based on neural networks. Kashiwagi and Tobi [13] also proposed a neural network algorithm for thermal load prediction. Ben-Nakhi and Mahmoud [14] used general regression neural networks and concluded that a properly designed neural network is a strong tool for optimizing thermal energy storage in buildings. Yao et al. [15] used a case study to show that a combined forecasting model based on a combination of neural networks and a few other methods is promising for predicting the hourly loads in buildings. Solmaz et al. [16] used the same concept of neural networks to predict the hourly cooling load for vehicle cabins.

Fuzzy logic and genetic algorithms are also used for developing predictor controllers. Sousa et al. [17] developed a fuzzy controller to be incorporated as a predictor in a nonlinear model-based predictive controller. Wang and Xu [18] used genetic algorithms to estimate the parameters of a building thermal network model using the operation data collected from site monitoring. They further combined a Resistance–Capacitance (RC) model of the building envelope with a data-driven approach where their RC parameters were corrected using real-time measurements [19].

The results of conventional load calculation methods can be improved by incorporating new mathematical algorithms that act on simple real-time measurements. Afram and Janabi-Sharifi [20] showed that improved load estimations can lead to the design and testing of more advanced controllers. It is shown that intelligent control based on thermal load prediction can maintain air quality while minimizing energy consumption [21]. By predicting thermal loads in real-time, controllers are not only capable of providing thermal comfort, but also adjusting the system operation to cope with upcoming conditions in an efficient manner [22].

Table 1 summarizes various characteristics of the available control methods for HVAC–R systems. These approaches cover a range including classic controllers to newer intelligent methods. In Table 1, 'Simplicity' refers to the ease of implementation of each method. 'Computational Intensity' determines the relative amount of on-site computational resources required for the algorithm to perform. 'Cost' is an indication of the relative cost of the method which is in relation to how commercially-available the method is, also indicated by 'Commercial Availability'. Different methods require different extents of system data such as the room thermal characteristics and the refrigeration cycle performance

Table 1
A summary of the characteristics of the available controller types for HVAC–R systems.

	On/off controller	PID controller	Neural network	Fuzzy logic	Genetic algorithm	Real-time load estimation
Sample reference	[10]	[9]	[12]	[17]	[18]	[20]
Simplicity	High	Medium	Low	Low	Low	Medium
Computational intensity	Low	Low	High	Medium	High	Medium
Cost	Low	Low	High	High	High	Medium
Commercial availability	High	High	Low	Low	Low	Low
System data requirement	Low	Medium	High	Medium	High	High
Prediction and adaptability	Low	Medium	High	Medium	High	High

information. The extent of such data required by each method is shown under 'System Data Requirement' in Table 1. Finally, 'Prediction and Adaptability' suggests how much every method is able to predict the upcoming thermal conditions and adapt the refrigeration cycle performance to the new scenarios.

A major drawback of the intelligent approaches is that they often tend to be mathematically complex and their implementation can be commercially unattractive in a range of regular applications. The sensors and computational resources required for the proper implementation of such intelligent methods may be unavailable for inexpensive systems. Furthermore, the usage of intelligent methods often presumes the availability of a variable-load refrigeration system that has variable-speed fans and compressor. Since many existing refrigeration systems are constant-load and only have on/off controllers installed, changing the set point values of the on/off controller as a means of improving energy efficiency can be a relatively effortless approach.

The output of an on/off controller is either on or off, with no middle state. To prevent damage to contactors and valves, an on/off 'hysteresis' is added to the controller operation [23]. This hysteresis causes the controller to wait for the temperature to surpass the set point by a certain amount before the output turns off or on again. As a result, on/off controllers practically have a pair of set points that are called the 'high set point' and the 'low set point'. Thus, the on/off controller of a cooling system keeps the system on until the temperature reaches the low set point. When this occurs, the system is switched off until the temperature rises back up to the high set point level, when it is switched on again. On/off hysteresis prevents the output from making fast, continual switches. With on/off controllers, a precise control of temperature is not achieved. However, the temperature keeps cycling or 'swinging' around the desired set point, resulting in an average temperature close to the desired set point.

Several researches have studied the optimization of on/off controllers. Chinnakani et al. [24] argued that a disadvantage of fixed gain PID control is that its performance can be poor under varying load conditions, so they developed an 'intelligent on/off controller' that takes into account sensor delays and room inertia. However, they assumed linear functionality for determining the slope of the temperature–time curves. Although the linear assumption is acceptable, assuming exponential functionality can be more accurate considering the form of the governing heat transfer equations. Li and Alleyne [10] presented an optimal compressor on/off control algorithm with a relay feedback loop. They developed a generic cost function involving temperature variation from the set-point, power consumption, and compressor on/off cycling frequency for minimization. The optimal control scheme was tested on a refrigeration system to demonstrate the potential of the optimal on/off control for temperature regulation, component wear reduction, and fuel consumption saving. They discussed the importance of the temperature swing periods in the action of on/off controllers and proposed a method for optimizing the high and low set points to minimize the cost function. However, they assumed that the temperature swing time periods have polynomial correlations with the set points, and calculated those parameters using simulation results rather than experiments. In the present study, it is proposed that exponential temperature correlations be used for the room thermal response. Moreover, the proposed set point optimization is based on experimental measurements without the necessity of further simulations.

In this study, the effect of hysteresis on the overall energy consumption is considered for the design of on/off HVAC–R controllers. It is shown through experiments that the average temperature, average power consumption, and the number of compressor starts per hour can be estimated using exponential correlations of the temperature data. A new mathematical model is developed based on the basic equations of the heat balance method. Current practice in the HVAC–R industry involves experimental tuning of the hysteresis value to maintain the desired threshold. However, in this study, formulations are proposed for properly selecting the high and low set point values in order to achieve the highest energy efficiency subject to the design constraints. The proposed approach is directly usable for the design of set points in all HVAC–R systems. In the following sections, the model development is described, followed by experimental results showing the energy-saving opportunities within the constraints of acceptable temperature deviation and number of compressor starts per hour.

2. Model development

An on/off controller of an HVAC–R system keeps the temperature swinging within a narrow range of temperatures called the

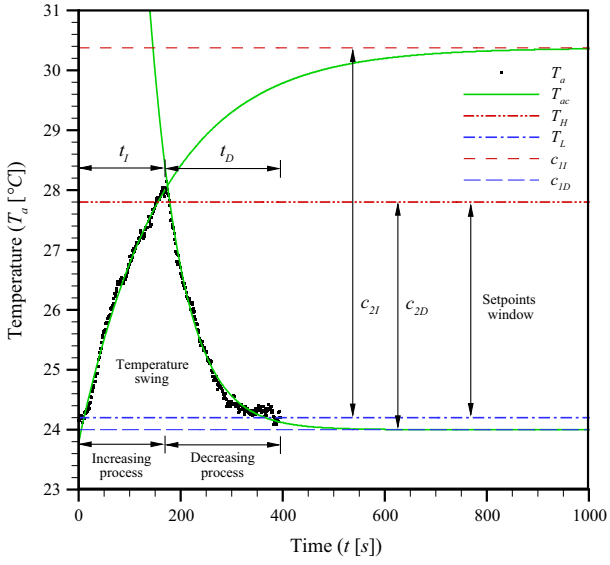

Fig. 1. Demonstration of a typical temperature pattern resulting from an HVAC–R on/off control action.

high set point T_H and the low set point T_L. Fig. 1 shows an example of a temperature swing in an air-conditioned system. In the example shown in Fig. 1, in order to maintain the temperature at 26 °C, the high and low set points are selected to be $T_H = 27.8$ °C and $T_L = 24.2$ °C, respectively. Therefore, starting from a low temperature, the air conditioning system is off and the room gains heat. This phenomenon results in the room temperature to increase, creating a temperature trend called an 'increasing process'. When the temperature reaches T_H, *i.e.*, the maximum allowable temperature, the AC system is turned on and the temperature begins to decrease. There is some lag in the process and a temperature overshoot is expected due to the thermal inertia of the room. This temperature overshoot is visible in Fig. 1 at the end of the increasing process denoted by time t_I. Afterwards, the refrigeration cycle works to pull down the room temperature during a period called the 'decreasing process' which lasts for time t_D. These processes occur consecutively in air conditioned and refrigerated spaces. Every two consecutive processes are called a 'temperature swing'. Useful information can be extracted from the study of temperature swings in any HVAC–R application [25].

The aim of the present model is to adopt a gray-box approach that will provide formulas for calculating energy-efficient set point values in HVAC–R on/off controllers. To combine the heat transfer equations with real-time data, the heat balance equation of a room envelop surrounded by walls numbered by i can be written as [26]:

$$m_a c_a \frac{dT_a}{dt} = \sum_i S_i h_i (T_{si} - T_a) + \dot{m}_v c_a (T_o - T_a) + \dot{Q}_g + \dot{Q}_{HVAC} \tag{1}$$

where

T_a is the homogeneous room air temperature and t is time;

$m_a c_a \frac{dT_a}{dt}$ is the rate of increase in the temperature of room air of mass m_a and specific heat c_a;

$\sum_i S_i h_i (T_{si} - T_a)$ is the convective heat transfer rate from surfaces S_i, with inside convection coefficients h_i, and inside surface temperatures T_{si};

$\dot{m}_v c_a (T_o - T_a)$ is the heat transfer rate due to air mass flow rate $\dot{m}_v$ from outside air temperature T_o by ventilation and infiltration;

$\dot{Q}_g$ is the convective heat flow gained from internal loads;

$\dot{Q}_{HVAC}$ is the heat flow to or from the HVAC system. It also includes any latent heat transfer due to condensation or evaporation.

Eq. (1) can be viewed as a differential equation with respect to the variable T_a. Rearranging Eq. (1), the following equation is achieved:

$$M \frac{dT_a}{dt} = -UT_a + H \tag{2}$$

where M, U, and H are positive values containing all the parameters included in Eq. (1). In general, these coefficients are also functions of T_a. M is a function of the air mass, the air specific heat, and the deep thermal mass of the objects inside the room. U is a function of the wall convective coefficients and the ventilation flow rate. H can also have a complicated dependency on the heat gain, HVAC load, outside temperature, and ventilation temperature.

The physical parameters included in M, U, and H are generally time-dependent. It is often necessary to gather information about the ambient conditions, the material properties, and the room's geometrical shape for estimating such parameters. However, when the room temperature is swinging between the set points, it has a relatively constant value. Therefore, most parameters such as the ambient temperature and ventilation rate have negligible variation and can be assumed constant. Although variations in the radiation load can occur in the room, these changes occur gradually compared to the small time span of a temperature swing. Therefore, it is reasonable to assume that all the parameters in Eq. (2) are constant during an instance of temperature swing. Any variation in the room conditions may still occur from one swing to the next, but as long as the swinging pattern is maintained, every parameter in Eq. (2) is assumed constant during a swing instance. Thus, the solution to the differential equation of Eq. (2) has the following exponential form:

$$T_{ac} = c_1 + c_2 \exp\left[-\frac{t - t_0}{c_3}\right] \tag{3}$$

where c_1, c_2, and c_3 are:

$$c_1 = \frac{H}{U} \tag{4}$$

$$c_2 = T_{a0} - \frac{H}{U} \tag{5}$$

$$c_3 = \frac{M}{U} \tag{6}$$

and t_0 and T_{a0} are the initial time and temperature of the specific process under consideration. T_{ac} is the correlated room air temperature. Eq. (3) is an exponential curve fit of the temperature variation during an increasing or decreasing process. The specific correlation for an increasing process has the following form:

$$T_{ac} = c_{1I} + c_{2I} \exp\left[-\frac{t - t_0}{c_{3I}}\right] \tag{7}$$

whereas the temperature correlation of a decreasing process has the following form:

$$T_{ac} = c_{1D} + c_{2D} \exp\left[-\frac{t - t_0}{c_{3D}}\right] \tag{8}$$

The subscript '*I*' denotes the parameters pertaining to an increasing process and '*D*' denotes the parameters of a decreasing process. Table 2 shows the physical interpretation of the correlations parameters.

The values of the c-parameters in Table 2 are unknown; they can be acquired through measurements. If the temperature in a room is recorded, Eqs. (7) and (8) can be used to fit exponential curves to the temperature values. After fitting exponential curves to the temperature data, the values of the c-parameters are found and they can be further used to assist the design and improvement of the controller set points. For every increasing or decreasing process, an exponential correlation can be found and a new set of c-parameters can be calculated.

Table 2
Physical interpretation of the c-parameters in the temperature correlation formula.

Parameter	Unit	Physical interpretation
c_{1I}	(°C)	Maximum steady-state room temperature reached in the current conditions if the cooling system is always off
c_{1D}	(°C)	Minimum steady-state room temperature reached in the current conditions if the cooling system is always on
c_{2I}	(°C)	Difference between c_{1I} and the low temperature set point ($T_L - c_{1I}$). c_{2I} is negative
c_{2D}	(°C)	Difference between c_{1D} and the high temperature set point ($T_H - c_{1D}$). c_{2D} is positive
c_{3I}	(s)	Time constant of the exponential temperature correlation for an increasing process, *i.e.*, the time required for the room temperature to cover 63% of its total increase and reach $T_a = c_{1I} + 0.37c_{2I}$ where c_{2I} is negative
c_{3D}	(s)	Time constant of the exponential temperature correlation for a decreasing process, *i.e.*, the time required for the room temperature to cover 63% of its total decrease and reach $T_a = c_{1D} + 0.37c_{2D}$ where c_{2D} is positive

An important aspect of the temperature swing patterns is the time span of each process. Rearranging Eq. (3) and using Eqs. (4) and (5), the time required for the room to reach temperature T_a through a process starting from $t = t_0$ and $T_a = T_{a0}$ is:

$$t - t_0 = c_3 \ln\left(\frac{T_{a0} - c_1}{T_a - c_1}\right) \tag{9}$$

In ideal conditions, every increasing process starts from $T_a = T_L$ and ends at $T_a = T_H$, while every decreasing process starts from $T_a = T_H$ and ends at $T_a = T_L$. Therefore, for an increasing process, the total time is:

$$t_I = c_{3I} \ln\left(\frac{T_L - c_{1I}}{T_H - c_{1I}}\right) \tag{10}$$

and for a decreasing process:

$$t_D = c_{3D} \ln\left(\frac{T_H - c_{1D}}{T_L - c_{1D}}\right) \tag{11}$$

where T_L and T_H are the low and high set points.

The temperature pattern during the entire operation of the system is merely a repetition of the swinging pattern. Therefore, the average swing temperature is equal to the overall average temperature, as long as the swinging pattern is maintained. As such, the average swing temperature is an important design objective. The average swing temperature is calculated by:

$$T_{mc} = \frac{\int_{t_I} T_a dt + \int_{t_D} T_a dt}{t_I + t_D} \tag{12}$$

where T_{mc} is the mean temperature calculated based on the temperature correlations. A temperature swing consists of an increasing process followed by a consecutive decreasing process. As such, for an entire temperature swing, using the correlations of Eqs. (7) and (8) for T_{ac}, and the definitions of Eqs. (10) and (11) for t_I and t_D, the following formulation is achieved:

$$T_{mc} = \frac{1}{t_I + t_D}\left[c_{1I}t_I + c_{1D}t_D + c_{2I}c_{3I} + c_{2D}c_{3D} - c_{2I}c_{3I}\exp\left(-\frac{t_I}{c_{3I}}\right) - c_{2D}c_{3D}\exp\left(-\frac{t_D}{c_{3D}}\right)\right] \tag{13}$$

It is required to keep the average temperature at the desired level via proper selection of the set points. Therefore, given either T_L or T_H, the other quantity can be found by implicitly solving Eq. (13) with t_I and t_D from Eqs. (10) and (11) so that the requirement for T_{mc} is met.

Another important parameter for the design of set point hysteresis is the overall power consumption. The compressor of the refrigeration cycle is off during increasing processes, and it is on during decreasing processes. When the compressor is on, its amount of power consumption depends on several factors such as air temperature, ambient temperature, and refrigerant pressure. However, within the narrow range of the set points, the compressor power can be assumed constant [25]. Therefore, the average compressor energy consumption per unit time is directly proportional to the amount of time that it is on. Assuming that the compressor consumes the power P_{comp} when it is on, the average power consumption over a swing period is calculated as:

$$P_{mc} = \frac{t_D}{t_I + t_D} P_{comp} \tag{14}$$

where P_{mc} is the average power consumption calculated based on the temperature correlations. Thus, proper selection of the set point levels directly affects the overall energy consumption through changing t_I and t_D in Eq. (14).

The number of compressor starts per hour is another important parameter in the design of refrigeration systems. Having found the process times t_I and t_D, the following relationship holds:

$$n_c = \frac{3600}{t_I + t_D} \tag{15}$$

where n_c is the estimated number of compressor starts per hour. Excessive compressor starts can reduce the lifetime of the compressor due to fatigue. It can also damage other components of the system including the valves and contactors. The increased current draw that happens at every new start also increases the total power consumption. A limit is often set by the manufacturers on the maximum allowable number of compressor starts per hour. As such, Eq. (15) can be used to design the set points subject to the constraint on the maximum allowable n_c.

The set of Eqs. (13)–(15) is crucial to the proposed method for selection of on/off set points. In the following section, a design strategy is described for using the present model as a tool for selecting the set points.

2.1. Design strategy

The optimization problem for selecting the on/off set points is formulated as minimizing the overall energy consumption subject to the following constraints:

- Minimum error between the average temperature and the desired temperature.
- Minimum temperature deviation from the desired temperature.
- Minimum number of compressor starts per hour.

The above constraints create competing trends for the selection of set points. Of course, there are specific obligations and preferences in every design case. For instance, minimizing the temperature deviation from the desired level may be critical in certain applications such as in refrigerated transportation of food products. In such a case, a higher number of compressor starts per hour may be acceptable as a sacrifice for selecting a narrow set point range. The present approach offers a design tool that can be flexibly used according to the needs of every specific engineering case.

The procedure for solving the optimization problem is as follows:

(1) Find the c-parameters by fitting the correlations of Eqs. (7) and (8) on temperature measurements.
(2) Decide upon the maximum allowable temperature deviation from the desired temperature.
(3) Decide upon the maximum allowable number of compressor starts per hour.
(4) Solve Eqs. (13) and (15) simultaneously for t_I and t_D subject to:
   - T_{mc} = Desired temperature.
   - n_c = Maximum allowable number of compressor starts per hour.
(5) Solve Eqs. (10) and (11) simultaneously for the minimum allowable T_H.
(6) Find the maximum allowable T_H based on the maximum allowable temperature deviation.
(7) Select the maximum suitable T_H within the range specified by steps 5 and 6.
(8) Find T_L for the selected T_H by solving Eq. (13) using Eqs. (10) and (11) for t_I and t_D, subject to:
   - T_{mc} = Desired temperature.

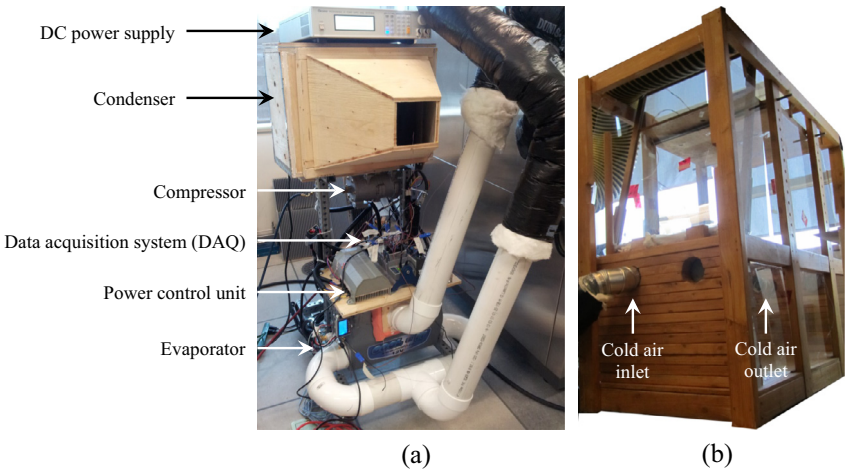

Fig. 2. (a) Air conditioning system. (b) Air-conditioned chamber.

(9) Estimate the optimized average power consumption using Eq. (14).
(10) Estimate the number of compressor starts per hour using Eq. (15).

In the following section, the model is validated by an experiment and the potentials for improving the overall energy efficiency are investigated.

3. Results and discussion

To test and verify the proposed model, a custom-designed testbed is built as shown in Fig. 2. The testbed is built out of wood, plastic, and glass, and is adjustable for testing a range of room dimensions and angles. There are two openings on the front and two on the rear walls of the chamber, as shown in Fig. 2b. Two of the openings are blocked and the other two are connected to the evaporator of an AC system.

Four T-type thermocouples (5SRTC-TT-T-30-36, Omega Engineering Inc., Laval, QC, Canada) are installed inside the chamber to measure the air temperature at several arbitrary locations. The thermocouples have an uncertainty of $\pm 1.0\,^{\circ}C$ and are connected to a data acquisition system (NI 9214DAQ, National Instruments Canada, Vaudreuil-Dorion, QC, Canada) for collecting the temperature values at a sampling rate of 1 Hz. However, one temperature value is sufficient to represent the chamber bulk temperature. The measured values of the thermocouples show a maximum standard deviation of $0.3\,^{\circ}C$ throughout the experiment. Therefore, it is ensured that the air temperature is uniform and the value of one of the thermocouples can represent the chamber bulk temperature with an acceptable deviation. Moreover, the standard deviation of $0.3\,^{\circ}C$ among the measurements ensures that the accuracy of $\pm 1.0\,^{\circ}C$ is compensated by comparing the data from the four thermocouples. Therefore, the measurements from one of the thermocouples are used as the chamber bulk air temperature in the model.

The chamber has the following overall dimensions: 150 cm high, 75 cm wide, 160 cm long. An electrical heater is placed inside the chamber at an arbitrary location. The heater is equipped with a fan to circulate air inside the chamber. The heater and its fan generate a total internal heat gain of $\dot{Q}_g = 641$ W. The instantaneous compressor power consumption varies between 490 W and 520 W when it is on. The amounts of power provided to the heater and compressor are controlled and monitored by two similar programmable DC power supplies (62012P-80-60, Chroma Systems Solutions Inc., Orange County, CA, US). According to the manufacturer datasheet, the maximum error of voltage and current measurements in the DC power supplies are $0.05\% + 0.05\%$ *F.S.* and $0.1\% + 0.1\%$ *F.S.*, respectively. *F.S.* is the full scale value of each quantity, *i.e.*, the maximum value deliverable by the equipment. The power is calculated in the power supplies by multiplying the voltage and current. Therefore, an uncertainty analysis of the experiments results in a maximum uncertainty of 0.4% for the power measurements.

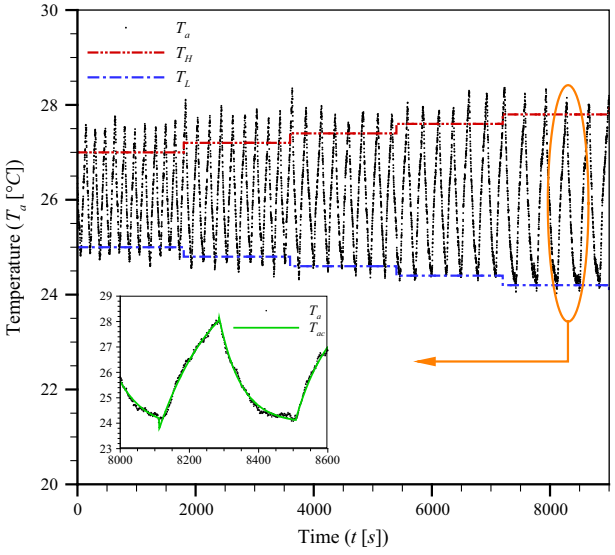

Fig. 3. Air temperature measurement results. Exponential correlations are applied with a minimum coefficient of determination of $R^2 = 0.98$.

The on/off controller switches the compressor on or off at the set point levels. However, the evaporator and condenser fans are always on during the tests. Every temperature swing consists of an increasing process, during which the compressor is off, followed by a decreasing process, during which the compressor is on. As discussed in the model development section, the compressor power can be assumed constant when it is operating within the narrow range of the set points. Therefore, according to the measurements, an average value of $P_{comp} = 497.7$ W is considered as the compressor power consumption.

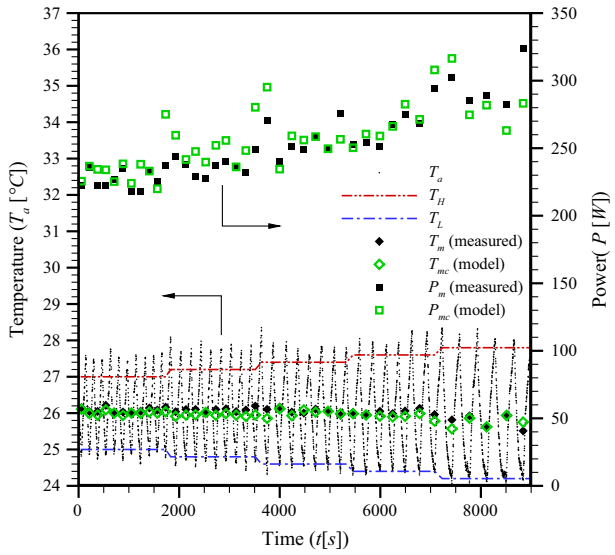

Fig. 4. Average temperature and power as measured and calculated using the exponential correlations. The maximum relative errors of average temperature and power are 1% and 16%, respectively.

3.1. Model validation

In a test designed for model validation, the high and low set points are varied every half an hour during the regular action of the refrigeration cycle connected to the chamber. An arbitrary value of 26 °C is selected as the desired temperature. A symmetric on/off set point hysteresis is selected, and its value is varied from ±1.0 °C to ±1.8 °C with increments of 0.2 °C at every 30 min. As such, the high set point varies from $T_H = 27.0$ °C up to $T_H = 27.8$ °C while the low set point varies from $T_L = 25.0$ °C down to $T_L = 24.2$ °C during an overall period of 150 min. The set points are applied by the data acquisition system based on the temperature feedback. Therefore, the measured temperature is compared with the selected set points and control commands are sent to the compressor accordingly.

Fig. 3 shows the temperature results throughout the 150 min (9000 s) of the refrigeration system's operation. T_a shows the air temperature as measured in the chamber. T_H and T_L are the high and low set points, respectively. At the bottom of Fig. 3, a zoomed-in view shows a single temperature swing with curve fits for T_{ac} using Eqs. (7) and (8). After identifying all the temperature swings, curve fits are applied to the increasing and decreasing processes of every swing instance separately. The minimum coefficient of determination for all the correlations is $R^2 = 0.98$.

In Fig. 3 it can be seen that the air temperature surpasses the high set point by up to 1 °C before it is pulled back down by the initiation of the cooling cycle's operation. There is also an overshoot at the low set point, but it is not as dramatic because the heat gains quickly increase the temperature once the cooling cycle is turned off. The surpassing of the air temperature beyond the set points is due to the chamber's thermal inertia as well as the residual cooling effect available in the evaporator after the compressor is turned off. As such, the set points create an approximate window of action for temperature control. The overshoot is less noticeable for larger hysteresis values, *i.e.*, to the right of Fig. 3. The temperature overshoot is often unavoidable in typical HVAC–R systems equipped with on/off controllers.

In the next step, the *c*-parameters for each temperature swing are found by applying the curve fits of Eqs. (7) and (8). The increasing time t_I and the decreasing time t_D are then calculated using Eqs. (10) and (11). The mean temperature and power consumption are calculated based on Eqs. (13) and (14). Since the average temperature and power calculated in this method are found based on the correlations, the subscript '*c*' is added to distinguish between the measured data and the calculated values.

Fig. 4 shows a comparison between the calculated average temperature T_{mc} and the measured average temperature T_m. The calculated average power P_{mc} is also compared with the measured average power P_m in Fig. 4. The measured mean temperature T_m is found by taking the average of the air temperature T_a over every swing period. The average power P_m is also calculated by taking the average of the measured compressor power over every temperature swing. Since the *c*-parameters correspond to the entire period of every temperature swing separately, the calculations are also performed for every swing. Therefore, T_m, T_{mc}, P_m, and P_{mc} are shown as discreet points at every swing occurrence. The maximum relative error for the calculation of mean temperature is 1%. The mean power consumption is calculated with a maximum relative error of 16%.

It is observed in Fig. 4 that, although the set points are symmetrically selected around the desired temperature of 26 °C, the measured average power can vary from $P_m = 217$ W up to $P_m = 323$ W. Therefore, it is shown in this experiment that improper selection of a symmetric set point hysteresis can remarkably affect the overall energy consumption. In this case, only selecting a hysteresis value of ±1.8 °C instead of ±1.0 °C increases the average power consumption by 49%. Moreover, the measured mean temperature is below the desired temperature of 26 °C in the larger hysteresis case. These issues are indications of the necessity for proper selection of set points.

As observed in Fig. 4, for higher values of symmetric hysteresis, the compressor needs to stay on during a larger portion of the temperature swings, *i.e.*, t_D increases more dramatically than t_I for higher hysteresis values. As a consequence, the average temperature decreases. In this test, although the desired temperature is set at 26.0 °C, mean temperatures as low as 25.5 °C are achieved for a hysteresis of ±1.8 °C. This proves that with selecting an improper pair of set points, the actual value of average temperature can be different from the desired temperature. In such cases, excessive cooling or heating is provided to the system which may not be necessary. Furthermore, high hysteresis values result

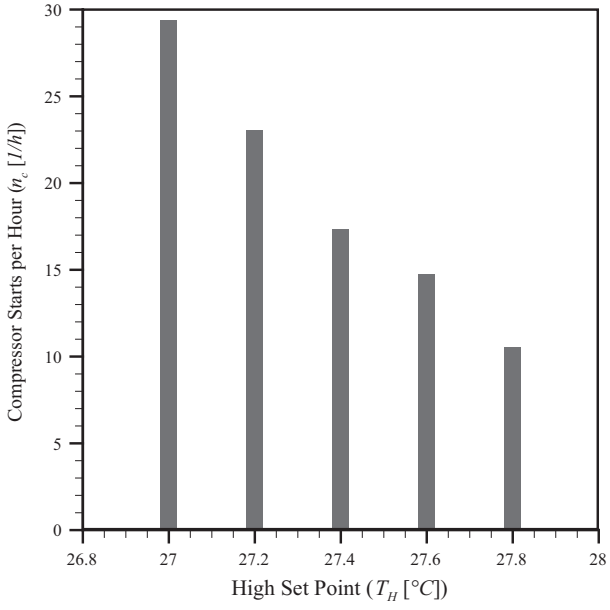

Fig. 5. Estimated number of compressor starts per hour for various set points.

in excessive temperature deviations from the desired value which may not be acceptable in certain applications.

Fig. 4 also shows the mean compressor power. As described above, the overall energy consumption increases with increasing symmetric hysteresis. Thus, when symmetric set points are to be selected around the desired temperature, it is preferable to choose narrower ones to avoid excessive temperature deviation and energy consumption. On the other hand, low hysteresis values result in high numbers of compressor starts per hour. Therefore, to avoid excessive compressor starts, the set points should not be too narrow.

Fig. 5 shows the estimated number of compressor starts per hour calculated by Eq. (15). As expected, increasing the gap between T_L and T_H results in decreasing n_c which is calculated based on the exponential temperature correlations. During every half-hour period when T_L and T_H are constant, the n_c values of different swing instances are almost equal to each other. But at the times when T_H and T_L change, the value of n_c also changes accordingly. Fig. 5 shows the average n_c calculated over the entire half-hour period of every set point pair.

The validated model can be used as a tool for set point design in any type of HVAC–R system equipped with an on/off controller. The proposed design strategy is utilized in the following section as a basis for energy-efficient design of set points in the present experiment.

3.2. Set point design

In this section, the design strategy outlined in the model development section is followed to select the set points for the experimental setup described above. It is necessary to find the *c*-parameters of the exponential correlations (step 1). Adopting a gray-box approach for an existing system, the *c*-parameters can be found by performing an experiment in which the room experiences a few swings. Then, the *c*-parameters can be used for analysis. In this example, the parameters listed in Table 3 are arbitrarily selected as they are found by piecewise correlations at $t = 4479$ s of the experiment shown in Fig. 3. Nevertheless, in an automatic system, the *c*-parameters can be updated at every swing, therefore providing more accurate parameters for the upcoming conditions.

The maximum allowable temperature deviation from the desired level is assumed to be 1.6 °C (step 2). The maximum number of compressor starts per hour is assumed to be 16 (step 3). The next step is to find the proper t_I and t_D for keeping the mean temperature at the desired level and n_c equal to the maximum allowable number of compressor starts per hour (step 4). Fig. 6 shows n_c versus T_H. For every value of T_H in Fig. 6, the corresponding T_L is calculated by solving Eq. (13) subject to T_{mc} equal to the desired temperature. Therefore, for every T_H, if T_L is correctly selected, T_{mc} is equal to the desired temperature and n_c can be found from Fig. 6. The minimum allowable T_H corresponding to $n_c = 16$ is thus estimated as 27.4 °C (step 5). On the other hand, the maximum allowable T_H is 27.6 °C, due to the decided maximum temperature deviation (step 6).

At this stage, the window of selection for T_H is found, *i.e.*, $27.4\ ^\circ\text{C} < T_H < 27.6\ ^\circ\text{C}$. Within this range, the number of compressor starts per hour and the temperature deviation are both less than their respective maximum allowable values. By proper selection of T_L for every T_H, the resulting mean temperature will also be equal to its desired value. Hence, all the constraints of the optimization problem are satisfied. The last stage of the design is to select a T_H value that minimizes P_{mc}. Fig. 7 shows the plot of the average power P_{mc} versus T_H, given that T_L is properly selected for every T_H so that T_{mc} is equal to the desired temperature of 26 °C. As observed in Fig. 7, the power consumption decreases with increasing T_H for this experiment. Therefore, the most energy-efficient value of T_H within its allowable range is $T_H = 27.6$ °C (step 7). By solving Eq. (13), the low set point is further found to be $T_L = 24.1$ °C, as also determined from Fig. 7 (step 8). The average power consumption can thus be calculated using Eq. (14) or Fig. 7 as $P_{mc} = 265.3$ W (step 9). The number of compressor starts per hour is also calculated using Eq. (15) or Fig. 6 as $n_c = 14$ starts per hour (step 10).

Table 3
c-parameters calculated at $t = 4479$ s of the experiment.

Parameter	Value	Parameter	Value
c_{1I}	29.9 °C	c_{1D}	22.3 °C
c_{2I}	−5.5 °C	c_{2D}	5.6 °C
c_{3I}	126 s	c_{3D}	128 s

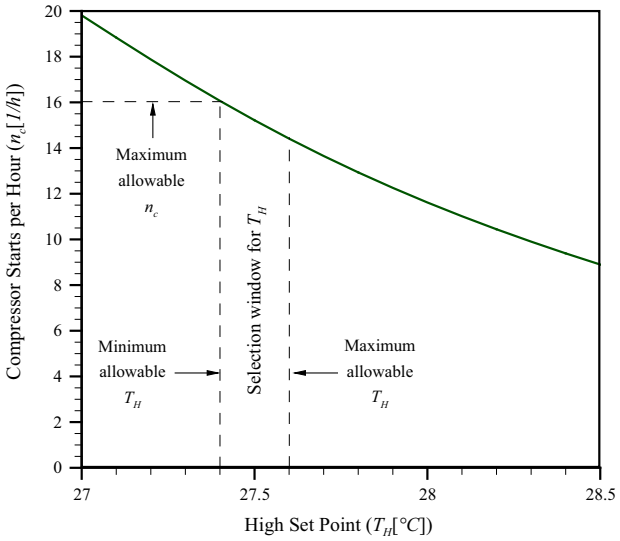

Fig. 6. Plot of n_c versus T_H given that T_L is properly selected to achieve $T_{mc} = 26$ °C at every T_H level.

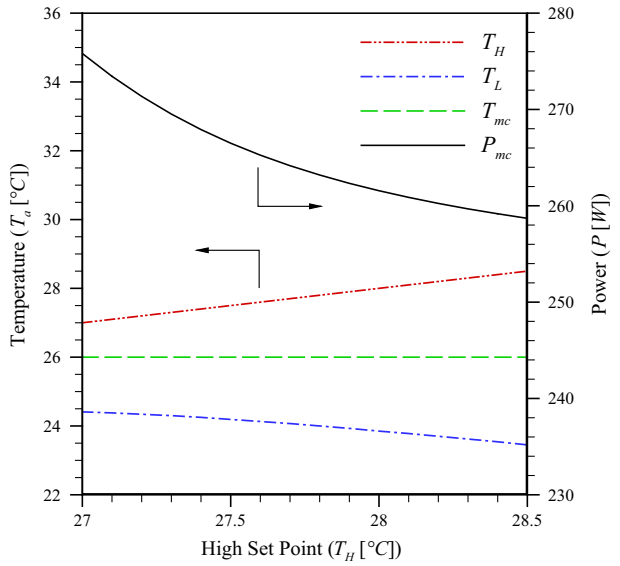

Fig. 7. Plot of P_{mc} versus T_H given that T_L is properly selected to achieve $T_{mc} = 26$ °C at every T_H level.

Fig. 7 shows that by selecting different set point pairs, the average power consumption for providing the same average temperature can vary from $P_{mc} = 275$ W down to $P_{mc} = 258$ W. Thus, a proper selection of asymmetric set points can save 6.6% of the overall energy. The slight decrease in the effective power consumption for higher hysteresis is because when the cycle is commanded to start at a higher T_H value, the cooling load provided to the chamber slightly increases. Hence, the higher temperature gradient between the chamber air and the cold air leads to a higher cooling effect for the same compressor power. Therefore, less overall energy is consumed by the cycle for the same mean temperature.

It should be noted that symmetric selection of hysteresis, as is done in Fig. 4, yields to different results compared with the asymmetric selection of set points according to the present model. Fig. 4 shows that if the set points are symmetrically selected around the desired temperature, larger hysteresis results in higher energy consumption. However, the mean temperature may not be equal to the desired value. As a result, more energy may be consumed to maintain an undesired average temperature. However, by selecting the set points by the present model, the average temperature is more accurately maintained at the desired level, and higher hysteresis yields to slightly less energy consumption.

The proposed design strategy forms an analytical tool for proper selection of the set points in any HVAC–R system equipped with an on/off controller. The prerequisite to using this method is to know the correlation parameters, an example of which is reported in Table 3. In order to find those parameters, it is necessary to have the temperature data for at least one temperature swing. Thus, the proposed method is readily applicable to existing systems. On the other hand, for new systems where the temperature data may not available, the proposed method can still be used by knowing the physical parameters of Eq. (1). Similar to white-box approaches, the designer can collect the physical and geometrical parameters of the governing equation. The proposed design strategy can then be used to reformulate the heat balance equation and utilize the resulting c-parameters for energy-efficient selection of on/off set points.

4. Conclusions

Many HVAC–R systems are equipped with on/off controllers. A high and a low set point are selected above and below the desired temperature to command the refrigeration cycle on or off. A design strategy is proposed in this study for energy-efficient selection of the set points. The objective is to select the set points for minimizing the overall energy consumption subject to the following constraints:

- Minimum error between the average temperature and the desired temperature.
- Minimum temperature deviation from the desired temperature.
- Minimum number of compressor starts per hour.

Following a gray-box approach, exponential correlations are fitted to raw temperature measurements. Based on the heat balance equation, the design strategy is formulated to provide analytical estimations of all the corresponding quantities. The model is validated by estimating the mean temperature and the average power consumption with maximum relative errors of 1% and 16%, respectively. It is experimentally shown that the set points can affect the overall energy consumption by as much as 49%, if they are symmetrically selected around the desired temperature. It is further shown that while maintaining the exact desired temperature, there is an opportunity to increase the energy efficiency by 6.6% using different high and low hysteresis values.

Acknowledgments

This work was supported by Automotive Partnership Canada (APC), Grant No. NSERC APCPJ/429698-11. The authors would like to thank the kind support of the Cool-It Group, 100-663 Sumas Way, Abbotsford, BC, Canada. The authors wish to acknowledge David Sticha for his efforts in building the testbed.

References

[1] Pérez-Lombard L, Ortiz J, Pout C. A review on buildings energy consumption information. Energy Build 2008;40(3):394–8.
[2] Chua KJ, Chou SK, Yang WM, Yan J. Achieving better energy-efficient air conditioning – a review of technologies and strategies. Appl Energy April 2013;104:87–104.
[3] Hovgaard T, Larsen L, Skovrup M, Jørgensen J. Power consumption in refrigeration systems-modeling for optimization. In: Proceedings of the 2011 4th international international symposium on advanced control of industrial processes; 2011. p. 234–39.
[4] Bagheri F, Fayazbakhsh MA, Thimmaiah PC, Bahrami M. Theoretical and experimental investigation into anti-idling A/C system for trucks. Energy Convers Manage 2015;98:173–83.
[5] Fayazbakhsh MA, Bahrami M. Comprehensive modeling of vehicle air conditioning loads using heat balance method. In: SAE transactions; 2013.
[6] Farrington R, Rugh J. Impact of vehicle air-conditioning on fuel economy, tailpipe emissions, and electric vehicle range. In: Earth technologies forum; 2000, no. September.
[7] Johnson VH. Fuel used for vehicle air conditioning: a state-by-state thermal comfort-based approach. SAE transactions; 2002.
[8] Li X, Wen J. Review of building energy modeling for control and operation. Renew Sustain Energy Rev September 2014;37:517–37.
[9] Wemhoff AP. Calibration of HVAC equipment PID coefficients for energy conservation. Energy Build February 2012;45:60–6.
[10] Bin Li BL, Alleyne AG. Optimal on-off control of an air conditioning and refrigeration system. In: American Control Conference (ACC), 2010; 2010. p. 5892–5897.
[11] Mirinejad H, Welch K, Spicer L. A review of intelligent control techniques in HVAC systems. Energytech, 2012 IEEE; 2010. p. 1–5.
[12] Li Q, Meng Q, Cai J, Yoshino H, Mochida A. Predicting hourly cooling load in the building: a comparison of support vector machine and different artificial neural networks. Energy Convers Manage January 2009;50(1):90–6.
[13] Kashiwagi N, Tobi T. Heating and cooling load prediction using a neural network system. In: Proceedings of 1993 international conference on neural networks (IJCNN-93-Nagoya, Japan), vol. 1; 1993. p. 939–42.
[14] Ben-Nakhi AE, Mahmoud MA. Cooling load prediction for buildings using general regression neural networks. Energy Convers Manage 2004;45(13–14):2127–41.
[15] Yao Y, Lian Z, Liu S, Hou Z. Hourly cooling load prediction by a combined forecasting model based on Analytic Hierarchy Process. Int J Therm Sci 2004;43(11):1107–18.
[16] Solmaz O, Ozgoren M, Aksoy MH. Hourly cooling load prediction of a vehicle in the southern region of Turkey by Artificial Neural Network. Energy Convers Manage 2014;82:177–87.
[17] Sousa JM, Babuška R, Verbruggen HB. Fuzzy predictive control applied to an air-conditioning system. Control Eng Practice 1997;5(10):1395–406.
[18] Wang S, Xu X. Parameter estimation of internal thermal mass of building dynamic models using genetic algorithm. Energy Convers Manage 2006;47(13–14):1927–41.
[19] Wang S, Xu X. Simplified building model for transient thermal performance estimation using GA-based parameter identification. Int J Therm Sci 2006;45(4):419–32.
[20] Afram A, Janabi-Sharifi F. Gray-box modeling and validation of residential HVAC system for control system design. Appl Energy January 2015;137:134–50.
[21] Khayyam H, Nahavandi S, Hu E, Kouzani A, Chonka A, Abawajy J, et al. Intelligent energy management control of vehicle air conditioning via look-ahead system. Appl Therm Eng 2011;31(16):3147–60.
[22] Khayyam H. Adaptive intelligent control of vehicle air conditioning system. Appl Therm Eng 2013;51(1–2):1154–61.
[23] Wang S, Ma Z. Supervisory and optimal control of building HVAC systems: a review. HVAC&R Res 2008;14:3–32. no. March 2015.
[24] Chinnakani K, Krishnamurthy A, Moyne J, Gu F. Comparison of energy consumption in HVAC systems using simple ON–OFF, intelligent ON–OFF and optimal controllers. In: IEEE Power and Energy Society General Meeting; 2011. p. 1–6.
[25] Fayazbakhsh MA, Bagheri F, Bahrami M. An inverse method for calculation of thermal inertia and heat gain in air conditioning and refrigeration systems. Appl Energy January 2015;138:496–504.
[26] Ghiaus C. Causality issue in the heat balance method for calculating the design heating and cooling load. Energy February 2013;50:292–301.